HHS Public Access

Author manuscript

Nature. Author manuscript; available in PMC 2017 August 02.

Published in final edited form as:

Nature. 2016 July 07; 535(7610): 153–158. doi:10.1038/nature18629.

Inflammasome - activated gasdermin D causes pyroptosis by forming membrane pores

Xing Liu[1,2,*], **Zhibin Zhang**[1,2,*], **Jianbin Ruan**[1,3,*], **Youdong Pan**[4], **Venkat Giri Magupalli**[1,3], **Hao Wu**[1,3], and **Judy Lieberman**[1,2]

[1]Program in Cellular and Molecular Medicine, Boston Children's Hospital, Boston, Massachusetts 02115, USA

[2]Department of Pediatrics, Harvard Medical School, Boston, Massachusetts 02115, USA

[3]Department of Biological Chemistry and Molecular Pharmacology, Harvard Medical School, Boston, Massachusetts 02115, USA

[4]Department of Dermatology and Harvard Skin Disease Research Center, Brigham and Women's Hospital, Boston, Massachusetts 02115, USA

Abstract

Inflammatory caspases (caspases 1, 4, 5 and 11) are activated in response to microbial infection and danger signals. When activated, they cleave mouse and human gasdermin D (GSDMD) after Asp276 and Asp275, respectively, to generate an N-terminal cleavage product (GSDMD-NT) that triggers inflammatory death (pyroptosis) and release of inflammatory cytokines such as interleukin-1β[1,2]. Cleavage removes the C-terminal fragment (GSDMD-CT), which is thought to fold back on GSDMD-NT to inhibit its activation. However, how GSDMD-NT causes cell death is unknown. Here we show that GSDMD-NT oligomerizes in membranes to form pores that are visible by electron microscopy. GSDMD-NT binds to phosphatidylinositol phosphates and phosphatidylserine (restricted to the cell membrane inner leaflet) and cardiolipin (present in the inner and outer leaflets of bacterial membranes). Mutation of four evolutionarily conserved basic residues blocks GSDMD-NT oligomerization, membrane binding, pore formation and pyroptosis. Because of its lipid-binding preferences, GSDMD-NT kills from within the cell, but does not harm neighbouring mammalian cells when it is released during pyroptosis. GSDMD-NT also kills cell-

---

Correspondence and requests for materials should be addressed to H.W. (wu@crystal.harvard.edu) or J.L. (judy.lieberman@childrens.harvard.edu).

*These authors contributed equally to this work.

Online Content Methods, along with any additional Extended Data display items and Source Data, are available in the online version of the paper; references unique to these sections appear only in the online paper.

Supplementary Information is available in the online version of the paper.

Author Contributions X.L. conceived the study. X.L., Z.Z., J.R., H.W. and J.L. designed the experiments and analysed the data. Experiments were performed as follows (X.L., Figs 1a–d, h, 2, 3a–d, 4a, c–f, h, Extended Data Fig. 1a–c, e, f; Z.Z. Figs 1e–g, 3b, d, Fig, 4b, e–h, Extended Data Fig. 1d; J.R. Figs 3, 4e, f; Y.P. Fig. 2e, f; V.M. Fig. 3e). X.L., H.W. and J.L. wrote the manuscript.

The authors declare no competing financial interests.

Readers are welcome to comment on the online version of the paper.

Reviewer Information *Nature* thanks F. Sigworth and the other anonymous reviewer(s) for their contribution to the peer review of this work.

free bacteria *in vitro* and may have a direct bactericidal effect within the cytosol of host cells, but the importance of direct bacterial killing in controlling *in vivo* infection remains to be determined.

We hypothesized that GSDMD-NT might form pores that permeabilize mammalian membranes during pyroptosis. To examine whether GSDMD-NT oligomerizes, we expressed Flag-tagged mouse GSDMD-NT or GSDMD in HEK293T cells and analysed the lysates by SDS–PAGE and Flag-immunoblot (Extended Data Fig. 1a, b). Under non-reducing conditions, GSDMD-NT migrated as both an ~30 kDa monomer and ≥250 kDa multimer. The multimeric band disappeared under reducing conditions, suggesting that GSDMD-NT oligomerization requires disulfide-cross-linking. Flag–GSDMD migrated mostly as a monomer, but a dimeric band was also formed when reactive sulfhydryl groups were not blocked, suggesting that these dimers formed during lysis. When the same cell lysates were analysed by native gel electrophoresis, high molecular weight oligomers were visualized selectively in cells transfected with Flag–GSDMD-NT (Fig. 1a). To confirm the association of multiple GSDMD-NT sub-units in the oligomer, we transfected HEK293T cells with Flag- and haemagglutinin (HA)-tagged GSDMD-NT. Immunoprecipitation with either anti-Flag (Fig. 1b) or anti-HA (Extended Data Fig. 1c) antibodies pulled down both tagged species, confirming that GSDMD-NT self- associates and might form homo-oligomers. When the co-immunoprecipitation was repeated in cells transfected with Flag–GSDMD-NT, Flag–GSDMD-CT, and/or GSDMD-CT–MYC, the two species of GSDMD-CT did not co-precipitate, but Flag–GSDMD-NT associated with MYC-tagged GSDMD-CT (Extended Data Fig. 1d).

Ectopic caspase-11 expression triggers pyroptosis in *GSDMD*-expressing cells[1,3]. To determine whether caspase-11 activates GSDMD cleavage and oligomerization, we co-transfected HEK293T cells, which do not express *GSDMD*, with plasmids encoding Flag–GSDMD and wild-type or enzymatically dead (C254A) caspase-11. We analysed cell death by measuring lactate dehydrogenase release and GSDMD oligomerization using SDS–PAGE and immunoblot, probed for Flag and caspase-11 (Fig. 1c). 60% of Flag–GSDMD-expressing cells co- expressing wild-type, but not mutant, caspase-11 were killed (Extended Data Fig. 1e). Only wild-type caspase-11 generated GSDMD-NT and its oligomer. Similar results were obtained when immortalized mouse bone-marrow-derived macrophages (iBMDMs) stably expressing Flag–GSDMD were electroporated with lipopolysaccharide (LPS) to activate caspase-11 (ref. 4; Fig. 1d, Extended Data Fig. 1f). Thus caspase-11 cleaves GSDMD, causing GSDMD-NT oligomerization and pyroptosis.

We hypothesized that GSDMD-NT oligomers form cell membrane pores that kill cells. Pore-forming proteins often use positively charged amphipathic structures for membrane insertion[5–7]. To identify potential functional pore domains, we searched for evolutionarily conserved, positively charged residues in GSDMD-NT, comparing the sequences of six mammalian species using the Clustal Omega and SOPMA secondary structure prediction server[8]. A cluster of four such residues occurs in a pair of predicted amphipathic α-helices (mouse Arg138, Lys146, Arg152, Arg154) (Fig. 1e, upper panel). Because of their possible importance, we engineered mutant forms of mouse Flag–GSDMD-NT containing 2, 3 or 4 Arg or Lys to Ala mutations of these residues. These changes were not predicted to affect the

secondary structure (Fig. 1e, lower panel), which was verified by showing that the melting temperatures of wild-type and 4 Ala (4A)-mutated GSDMD-NT were similar (46.8°C and 45.6°C, respectively). We also generated a mutant protein in which Arg138 was mutated to Ser. We determined whether these mutations interfere with oligomerization and pyroptosis in HEK293T cells ectopically expressing GSDMD, wild-type or mutated GSDMD-NT (Fig. 1f, g). As expected, wild-type GSDMD-NT, but not GSDMD, triggered both pyroptosis and GSDMD-NT oligomerization. Mutation of all four basic residues completely blocked both pyroptosis and oligomerization, whereas mutations of two or three of the residues resulted in partial blocking. Ectopic Flag- and HA-tagged GSDMD-NT 4A also did not co-immunoprecipitate (Extended Data Fig. 2a). Ala mutations of other conserved basic residues (Lys204, Lys205, Lys237, Arg239), alone or combined with mutations in nonconserved basic residues (Arg248, Lys 249) that were not within predicted amphipathic structures, did not affect pyroptosis (Extended Data Fig. 2b, data not shown). Oligomerization and cell death were correlated, suggesting that GSDMD-NT oligomers were responsible for pyroptosis.

To verify that the 4A mutation inactivates pyroptosis, we knocked down *Gsdmd* in iBMDMs and assessed whether wild-type or 4A-mutant GSDMD restored LPS-transfection-induced pyroptosis (Fig. 1h, Extended Data Fig. 2c, d). *Gsdmd* knockdown strongly inhibited pyroptosis, which was restored by ectopic expression of small interfering RNA (siRNA)-resistant wild-type, but not 4A mutant, *Gsdmd*.

Because GSDMD-NT oligomerization was inhibited by reducing agents, we also mutated the six Cys residues in the mouse protein and analysed oligomerization in transfected cells. Mutations of Cys39 or Cys192 impaired oligomerization, suggesting that intramolecular or intermolecular disulfide bonds between these residues are critical for oligomerization (Extended Data Fig. 2e).

If GSDMD-NT forms plasma membrane pores, it should relocalize to the cell membrane after caspase activation. To assess membrane localization, we lysed cells co-transfected with wild-type or 4A Flag–GSDMD and wild-type or C254A caspase-11 in the detergent Triton X-114 to separate cytosolic proteins in the aqueous phase from membrane-associated proteins in the detergent phase[9] (Fig. 2a, b). A cleavage fragment that migrated in the same way as Flag–GSDMD-NT was only produced in cells transfected with wild-type caspase-11. Wild-type and 4A Flag–GSDMD-NT were detected in the aqueous phase, but only wild-type Flag–GSDMD-NT partitioned into the detergent phase and associated with cell membranes.

To determine with which membrane GSDMD-NT associates, we fractionated the post-nuclear supernatant of HEK293T cells, transfected with Flag–GSDMD, or wild-type or 4A GSDMD-NT expression plasmids, into cytosolic (S100), heavy membrane (P7), light membrane (P20) and insoluble cytoplasmic fractions (P100) (Fig. 2c). Flag–GSDMD and 4A GSDMD-NT were solely in the S100 fraction, but Flag–GSDMD-NT fractionated with both the S100 and heavy membrane P7 fraction, which contains plasma-membrane fragments and mitochondria. When HEK293T cells, transfected to express Flag–GSDMD-NT, were separated into soluble and membrane fractions and analysed by immunoblot, the cytosolic fraction contained mostly monomeric Flag–GSDMD-NT, whereas the membrane

fraction only contained the high molecular weight oligomer (Fig. 2d). We used confocal immunofluorescence microscopy to visualize the cellular distribution of transiently expressed Flag-tagged GSDMD and wild-type and 4A-mutant GSDMD-NT (Fig. 2e, f). Flag–GSDMD and oligomerization-defective 4A Flag–GSDMD-NT stained the cytosol diffusely, but Flag–GSDMD-NT concentrated on the plasma membrane. Thus, GSDMD-NT oligomerizes in the plasma membrane during pyroptosis.

Lipid binding influences which membranes pore-forming proteins permeabilize. To identify which lipids GSDMD-NT binds, we incubated recombinant GSDMD, GSDMD-NT, GSDMD-CT and 4A GSDMD-NT and the cytotoxic lymphocyte pore-forming proteins, perforin and granulysin, with membranes dotted with different lipids (Fig. 3a, b). Perforin permeabilizes mammalian membranes, whereas granulysin preferentially permeabilizes microbial membranes[10,11]. Consistent with our previous results, GSDMD, GSDMD-CT and 4A GSDMD-NT did not bind to any lipid. GSDMD-NT bound most strongly to the mitochondrial and bacterial lipid, cardiolipin, and to the phosphatidylinositol phosphates (PIPs), PtdIns(4)P and PtdIns(4,5) P2, and less strongly to phosphatidic acid (PA) and phosphatidylserine (PS), which are all on the mammalian cell membrane inner leaflet[12,13]. It did not bind to phosphatidylethanolamine (PE) or phosphatidylcholine (PC), the major lipids on both plasma membrane leaflets. Cardiolipin in the mitochondrial inner membrane is inaccessible to the cytosol[14]. This binding pattern suggests that GSDMS-NT may selectively bind to the plasma membrane from within and to bacterial membranes. The outer leaflet of endosome and phagosome membranes contains the same phospholipids as the plasma membrane inner leaflet, suggesting that GSDMD-NT may also bind to these organelles. In comparison, perforin bound to PE, but not PS, and the same PIPs as GSDMD-NT, consistent with its role in permeabilizing mammalian cell membranes from the outside; granulysin also bound to cardiolipin, consistent with its role in microbial immunity. Mixed lineage kinase domain-like protein, the pore-forming protein activated during necroptosis, which binds to the inner leaflet of the cell membrane, has a similar binding pattern as GSDMD-NT[15–18].

To confirm lipid binding by GSDMD-NT, we measured wild-type and 4A-mutant GSDMD-NT binding and disruption of PE–PC liposomes containing no added lipid or PtdIns(4)P, PtdIns(4,5)P2, PS or PA (Fig. 3c, d). 4A GSDMD-NT did not bind any of these liposomes, whereas wild-type GSDMD-NT bound to all of the liposomes containing the added phospholipids, but not to the PE–PC liposomes. To measure liposome leakage, PE–PC–PS liposomes were prepared that encapsulated Tb^{3+} ions. Alone, Tb^{3+} is weakly fluorescent, but fluoresces strongly when bound to dipicolinic acid (DPA)[19]. Fluorescence of PE–PC–PS liposomes in DPA-containing solutions sharply increased after adding wild-type, but not mutant, GSDMD-NT, indicating Tb^{3+} leakage. Similarly, PS-containing liposomes became leaky after incubation with caspase-11-treated GSDMD, but not after incubation with caspase-11 or GSDMD alone. Thus GSDMD-NT binds to liposomes containing PS or PIPs and disrupts them. The buffer used for these experiments is Ca^{++}-free, suggesting that GSDMD-NT oligomerization, unlike perforin oligomerization, is Ca^{++}-independent.

We next used negative staining electron microscopy to visualize GSDMD-NT oligomers on PS-containing liposomes. Liposomes incubated with GSDMD and caspase-11 showed ruptured morphology, whereas those incubated with only GSDMD did not (Fig. 3e). The

ruptured liposomes were decorated with neck-like structures with ~30nm diameters at membrane openings, which may represent side views of GSDMD-NT pores. To visualize these potential pore-like structures top-down, we used detergent to extract the reconstituted pores from liposomes and purified the proteins through a size-exclusion column before performing negative staining electron microscopy. Stable ring structures with ~15 nm inner and ~32 nm outer diameters were observed, but only when both caspase-11 and GSDMD were added (Fig. 3f). Cleaved interleukin-1β, released from cells undergoing pyroptosis[20], has a diameter of ~4.5nm (ref. 21) and could readily pass through these pores.

Pyroptotic cells release cytosolic contents into the surrounding media[22]. We used Flag immunoblot to determine whether pyroptotic HEK293T cells ectopically expressing Flag–GSDMD-NT release GSDMD-NT into the culture medium (Fig. 4a). Whereas ectopic Flag–GSDMD was only detected in the cell, Flag–GSDMD-NT was mostly detected in culture supernatants. To examine the activity of released GSDMD-NT, we assessed iBMDM viability after incubation with fivefold-concentrated culture supernatants from HEK293T cells ectopically expressing Flag–GSDMD-NT or Flag–GSDMD (Extended Data Fig. 3a). Neither supernatant killed iBMDMs. These results were confirmed by examining propidium iodide uptake of CFSE-labelled untransfected HEK293T cells after incubation with Flag–GSDMD-NT-expressing HEK293T cells (Extended Data Fig. 3b). Virtually all of the transfected cells died, but none of the bystander cells, consistent with previous reports[2,23]. Thus GSDMD-NT does not injure bystander cells—it does not disrupt the plasma membrane from the outside, which is expected as it only binds to phospholipids present on the inner leaflet of the plasma membrane of viable cells (Fig. 3a, b).

As GSDMD-NT also binds to cardiolipin, we investigated whether the concentrated pyroptotic cell supernatant kills bacteria (Fig. 4b). The pyroptotic supernatant reduced *Escherichia coli* colonies in a dose- dependent manner. As pyroptotic cell supernatants contain many antibacterial factors, including lysosomal enzymes and lysozyme, we assessed the anti-bacterial activity of culture supernatants that were immunodepleted of Flag–GSDMD-NT (Fig. 4c). Depletion of GSDMD-NT inhibited bacterial killing, supporting a direct antibacterial effect of GSDMD-NT. These culture supernatants were concentrated from cells overexpressing GSDMD-NT, an unphysiological condition that might have unnaturally exaggerated bacterial killing. To examine whether enough endogenous GSDMD-NT is released to kill extracellular bacteria, we collected antibiotic-free culture supernatants from iBMDMs, transfected with LPS or control Pam3CSK4 or treated with LPS and nigericin for 3 h, and added them at dilutions of 1:4 or 1:2 to *Listeria monocytogenes*. Addition of unconcentrated pyroptotic iBMDM culture supernatants significantly reduced bacterial colony-forming units (c.f.u.) in a dose-dependent manner (Fig. 4d).

To confirm that GSDMD-NT accounts for the anti-bacterial activity, we measured *E. coli* and *Staphylococcus aureus* c.f.u. after incubation with nanomolar concentrations of recombinant GSDMD, GSDMD-CT, wild-type or 4A GSDMD-NT, or granulysin (Fig. 4e). Wild-type GSDMD-NT strongly inhibited colony formation of both bacteria, but the other GSDMD constructs had no anti-bacterial activity. Moreover GSDMD-NT was more active than granulysin. The anti-bacterial effect was rapid: after only 5 min, bacterial c.f.u. were

reduced ~2-fold (Fig. 4f). Bacterial growth measurements after treatment with the GSDMD proteins confirmed these results (Extended Data Fig. 3c). To determine whether GSDMD-NT is bactericidal, we measured propidium iodide uptake by *E. coli* and *L. monocytogenes* after treatment for 20 min with the same GSDMD constructs (Extended Data Fig. 3d, data not shown). Wild-type GSDMD-NT killed ~80% of bacteria, but 4A GSDMD-NT, GSDMD-CT and GSDMD had no effect. We next used spinning disk fluorescence microscopy to visualize whether AlexaFluor-488-labelled GSDMD-CT or GSDMD, treated or not with caspase-11, bound to mCherry-expressing *L. monocytogenes* (Extended Data Fig. 3e). Only caspase-11-treated GSDMD bound. Thus GSDMD-NT, released from pyroptotic cells, rapidly binds to and kills both Gram-negative and Gram-positive bacteria.

Intracellular bacteria trigger pyroptosis when LPS on cytosolic Gram-negative bacteria activates the noncanonical inflammasome or when invasive Gram-negative or -positive bacteria activate the canonical inflammasome[4,24–28]. We first looked at whether ectopic GSDMD or wild-type or 4A-mutant GSDMD-NT kills intracellular *L. monocytogenes* in HeLa cells (Fig. 4g). HeLa cells were infected 6 h after transfection. Although expression of GSDMD or 4A GSDMD-NT had no effect, wild-type GSDMD-NT significantly reduced recovery of viable bacteria 6 h and 12 h later. To assess whether cleavage of endogenous GSDMD induces intracellular bacterial killing, we examined the effect of inflammasome activation on the survival of intracellular *L. monocytogenes* in iBMDMs. When LPS-primed-iBMDMs infected with *L. monocytogenes* were treated with nigericin for 1 h to activate the canonical inflammasome, bacterial c.f.u. were reduced ~2-fold (Fig. 4h). Infection of iBMDMs with *L. monocytogenes* also independently triggers AIM2/ASC/caspase-1-mediated pyroptosis[28]. To assess the importance of GSDMD-NT bacterial killing by direct listerial inflammasome activation, we examined the effect of *Gsdmd* knockdown on bacterial c.f.u. (Fig. 4i). iBMDMs with *Gsdmd* knocked down contained threefold more bacteria, indicating that inflammasome activation in infected cells causes GSDMD-dependent death of intracellular bacteria. The intracellular infection experiments (Fig. 4g–i) were performed without antibiotics, but similar results were obtained when gentamicin was used to kill extracellular bacteria and removed before triggering pyroptosis (data not shown). Thus, inflammasome activation of GSDMD kills both intracellular and extracellular bacteria *in vitro*. However, viable bacteria were not completely eliminated from these cultures. GSDMD-NT could reduce intracellular bacteria by causing host cell death, expelling bacteria from the intracellular niche that is favourable for their survival and replication[29], or by a direct anti-bacterial effect. We have no experimental method to dissociate eukaryotic cell death from bacterial cell death at this time.

How inflammatory caspase cleavage of GSDMD causes pyroptosis[1,2] was previously unknown. Here we show that GSDMD-NT binds to membranes containing PS, cardiolipin, or PIPs to form oligomeric pores that kill mammalian cells and the bacteria that trigger pyroptosis. GSDMD-NT is released into the extracellular milieu during pyroptosis. Because GSDMD-NT binds selectively to phospholipids that are restricted to the inner leaflet of mammalian cell membranes, GSDMD-NT does not kill bystander cells. This selective activity should control tissue damage. GSDMD-NT killing of intracellular bacteria should limit the release of viable bacteria from pyroptotic cells and reduce the spread of infection. We do not know whether GSDMD-NT is active only against bacteria that have escaped from

the phagosome. Because the phagosome outer leaflet derives from the inner leaflet of the plasma membrane, phagosomes could be targeted by GSDMD-NT, providing a mechanism for lysis of bacteria within phagosomes. Released GSDMD-NT is active on extracellular bacteria, which probably also helps to control infection. *In vivo* experiments to show that GSDMD-mediated bacterial pore formation protects against bacterial infection would be needed to determine whether direct bacterial killing is physiologically important. However, we do not have a way to distinguish *in vivo* direct killing of bacteria from killing of the host cell (pyroptosis), as the mechanisms that disrupt one also disrupt the other.

A better understanding of how GSDMD-NT forms pores and a more complete description of the GSDMD-NT pore could be obtained by solving the structures of monomeric and oligomerized GSDMD-NT. The oligomers formed in cells overexpressing GSDMD-NT on native gels (Fig. 1a) appeared to be heterogeneous in size, whereas the purified reconstituted pores (Fig. 3f) appeared homogeneous. Direct visualization of the pores formed on cellular membranes should determine whether the pores are uniform. Our identification of mutations that inactivate pore formation, but probably do not affect its overall structure, should help to assess the importance of GSDMD-NT pores in controlling *in vivo* infection.

METHODS

Data reporting

No statistical methods were used to predetermine sample size. The experiments were not randomized and the investigators were not blinded to outcome assessment.

Cell lines and bacterial strains

HEK293T and HeLa cells were obtained from ATCC, and C57BL/6 mouse iBMDM cells were provided by J. Kagan (Boston Children's Hospital). Cells were cultured in DMEM (Invitrogen) with 10% heat- inactivated foetal bovine serum, supplemented with 100 U ml^{-1} penicillin G, 100 μgml^{-1} streptomycin sulphate, 6 mM HEPES, 1.6 mM L-glutamine, and 50 μM 2-mercaptoethanol (2ME). There were no antibiotics in the cell culture medium used for bacterial infection and for experiments in which culture supernatants were collected for bacterial incubation. Cells were verified to be free of mycoplasma contamination. Transient transfection of HEK293T and HeLa cells was performed using the calcium phosphate method or Lipofectamine 2000 (Invitrogen) according to the manufacturer's instructions. iBMDM cells were transfected by nucleofection (Amaxa) using the Amaxa Nucleofector kit (VPA-1009). Bacterial strains were obtained from ATCC (*E. coli* strain BL21, *S. aureus* strain CA-MRSA USA300 and *L. monocytogenes* 10403S strain) and grown in Luria broth (LB), tryptic soy broth and brain–heart infusion media, respectively.

Reagents

Polyclonal anti-human GSDMD was from Novus Biologicals (NBP2-33422) or Proteintech (20770-1-AP). Monoclonal anti-haemagglutinin (F-7) antibody (sc-7392) was from Santa Cruz Biotechnology. Monoclonal anti-Flag M2 antibody (F1804), monoclonal anti-human α-tubulin antibody (T5168) and monoclonal anti-mouse caspase-11 antibody (C1354) were from Sigma-Aldrich. Polyclonal anti-human Na^+/K^+-ATPase α1 (ATP1A1) antibody

(#3010) was from Cell Signaling. c-MYC (9E10) monoclonal antibody (MMS-15P) was from Covance. Monoclonal anti-human perforin antibody (3465-6-250) and polyclonal anti-human granulysin antibody (AF3138) were from Mabtech and Novus, respectively. *N*-ethylmaleimide, 2ME, DTT, terbium(III) chloride, DPA (dipicolinic acid) and nigericin were from Sigma-Aldrich. Ultrapure LPS and Pam3CSK4 were from InvivoGen. The complete protease inhibitor cocktail was from Roche. siRNA duplexes targeting *Gsdmd* (s87492; 5′-GGUGAACAUCGGAAAGAUUTT-3′) and the nonspecific control siRNA (CTL, 4390843) were from Ambion.

Plasmids

pCMV6-*Gsdmd* and pCMV-Flag-caspase-11 constructs were obtained from Origene and Addgene, respectively. cDNA for *Gsdmd* was subcloned into pFlag-CMV4, pcDNA3-N-HA and pcDNA3-C-5xMyc. GSDMD truncation mutants were derived by PCR from the corresponding plasmids. All point mutations were generated using QuikChange XL site-directed mutagenesis (Stratagene). All plasmids were verified by sequencing.

Protein expression and purification

Full-length human GSDMD was cloned into the pDB.His.MBP vector with a tomato etch virus (TEV)-cleavable N-terminal His_6-MBP tag using NdeI and Xho I restriction sites. 4A GSDMD, GSDMD-CT, and wild-type and 4A-mutant GSDMD were constructed by QuikChange Mutagenesis (Agilent Technologies). For expression and purification of full-length GSDMD, GSDMD-CT and GSDMD-NT 4A mutant, *E. coli* BL21 (DE3) cells harbouring the indicated plasmids were grown in LB medium supplemented with 50 μg ml^{-1} kanamycin. Protein expression was induced at 18°C overnight by 0.5 mM isopropyl-β-D-thiogalactopyranoside (IPTG) when OD_{600} reached 0.8. Cells were collected and resuspended in lysis buffer containing 25 mM Tris-HCl (pH 8.0), 150 mM NaCl, 20 mM imidazole and 5 mM 2ME, and lysates were homogenized by ultrasonication. The cell lysate was clarified by centrifugation at 40,000*g* at 4°C for 1 h. The supernatant containing the target protein was incubated with Ni-NTA resin (Qiagen) that was pre-equilibrated with lysis buffer for 30 min at 4°C. After incubation, the resin–supernatant mixture was poured into a column and the resin was washed with lysis buffer. The protein was eluted using the lysis buffer supplemented with 500 mM imidazole. The His_6-MBP-tagged protein was further purified by HiTrap Q ion-exchange and Superdex 200 gel-filtration chromatography (GE Healthcare Life Sciences). The His_6-MBP tag was removed by overnight TEV protease digestion at 16°C. The cleaved protein was purified using HiTrap Q ion-exchange and Superdex 200 gel-filtration columns.

The yield of wild-type GSDMD-NT was lower than for the other constructs because it inserted into bacterial membranes and killed >50% of bacteria after overnight expression, and thus required a different purification strategy. To purify wild-type GSDMD-NT, cells containing the pDB-His_6-MBP-GSDMD-NT clones were grown and induced as described for full-length GSDMD. They were collected and resuspended in lysis buffer containing 25 mM Tris-HCl (pH 8.0) and 150 mM NaCl, and homogenized by ultrasonication. The membrane fraction was harvested by ultracentrifugation at 200,000*g* at 4°C for 1 h and resuspended and solubilized with 1.0% *n*-dodecyl-β-D-maltoside (DDM) in lysis buffer

supplemented with 20 mM imidazole using a glass homogenizer, followed by centrifugation at 200,000*g* at 4°C for 45 min. The supernatant containing the solubilized protein was incubated for 30 min at 4°C with Ni-NTA resin (Qiagen) that was pre-equilibrated with the lysis buffer containing 1% DDM and 20 mM imidazole. The resin was washed with lysis buffer containing 1% DDM and 20 mM imidazole, and the recombinant proteins were eluted with lysis buffer supplemented with 500 mM imidazole and 0.1% DDM. The His_6-MBP-GSDMD-NT protein was further purified using a Superdex 200 gel-filtration column. For protein used for bacterial growth assay, the Ni-NTA resin was washed with at least 40 column volumes of lysis buffer without detergent before elution and the protein was further purified with detergent-free buffers.

The caspase-11 gene was cloned into the pFastBac-HTa vector with a TEV cleavable N-terminal His_6-tag using EcoRI and XhoI restriction sites. The baculoviruses were prepared using the Bac-to-Bac system (Invitrogen), and the protein was expressed in Sf9 cells following the manufacturer's instructions. His–caspase-11 baculovirus (10 ml) was used to infect 1 l of Sf9 cells. Cells were collected 48 h after infection and His–caspase-11 was purified following the same protocol as for His_6-MBP–GSDMD. After elution from Ni-NTA resin, the protein was further purified using a Superdex 200 gel-filtration column. Aggregated fractions, which were the activated form of caspase-11, were collected for use in subsequent assays. For some experiments GSDMD-NT was generated by mixing caspase-11 with GSDMD at a 1:3 mass ratio for indicated times at 16°C.

Native human granulysin and perforin were purified from isolated YT-Indy cytotoxic granules as previously described[30].

GSDMD thermal shift assay

Experimental protein unfolding was monitored by fluorescence of the Protein Thermal Shift Dye (Thermo Fisher Scientific) as temperature was continuously increased at a ramp rate of 1.6°C per min using an Applied Biosystems StepOne Real-Time PCR machine. Samples of wild-type and 4A-mutant MBP–GSDMD were subdivided into three 20 μl replicates on a MicroAmp Optical 96-Well reaction plate. The transition thermal melting temperatures (T_m) were extracted using Applied Biosystems StepOne software version 2.3.

Immunoblot and immunoprecipitation

Cells were lysed in lysis buffer (50 mM Tris-Cl (pH 7.4), 150 mM NaCl) supplemented with 1% Triton-X100, 1 mM PMSF. Cell lysates were boiled in SDS loading buffer for 5 min before electrophoresis through SDS–PAGE gel. The resolved proteins were then transferred to a polyvinylidene difluoride (PVDF) membrane (Millipore), which was probed with the indicated antibodies. Protein bands were visualized using a SuperSignal West Pico chemiluminescence ECL kit (Pierce). For non-reducing gels, cells were lysed in lysis buffer with or without 30 mM *N*-ethylmaleimide and cell lysates were prepared with 2ME-free SDS loading buffer. For immunoprecipitations, cell extracts were prepared using RIPA buffer (50 mM Tris-HCl (pH 7.4), 150 mM NaCl, 1 mM EDTA, 1% Triton X-100, 0.1% SDS, 0.5% deoxycholate) containing complete protease inhibitor cocktail. Lysates were incubated with the relevant antibody for 4 h at 4°C before adding protein A/G agarose for 2

h. Beads were washed three times with the same buffer and bound proteins were eluted with SDS loading buffer by boiling for 5 min.

Native gel immunoblot

Cells samples, prepared using NativePAGE Sample Prep Kit (Invitrogen), were electrophoresed through a 4–16% NativePAGE Bis-Tris gel (Invitrogen) in NativePAGE running buffer (Invitrogen) at 4°C and 150 V. Proteins were then transferred to a PVDF membrane at 0.2 A for 1 h in NativePAGE transfer buffer (Invitrogen) for immunoblotting.

Cytotoxicity assays

Cell death and cell viability were determined by the lactate dehydrogenase release assay using CytoTox 96 Non-Radioactive Cytotoxicity Assay kit (Promega) and by measuring ATP levels using the CellTiter-Glo Luminescent Cell Viability Assay (Promega), respectively, according to the manufacturer's instructions.

Triton X-114 phase separation

Cells were lysed in lysis buffer (20mM HEPES (pH7.4), 150 mM NaCl, 2% Triton X-114 (Sigma), complete protease inhibitor) and then centrifuged at 15,000*g* for 15 min. The resultant supernatant mixture was incubated at 30°C for 10 min to separate the upper aqueous fraction from the lower detergent soluble fraction. The aqueous fraction was spun at 1,500*g* for 5 min at room temperature and the upper fraction harvested to eliminate contamination from the detergent-enriched phase. The detergent-enriched phase was diluted with lysis buffer lacking Triton X-114 and re-spun at 1,500*g* for 10 min and the detergent phase was recollected. The washed detergent phase was diluted with lysis buffer lacking Triton X-114 to the same final volume as the aqueous faction.

Cell fractionation

Cells were washed with PBS and collected by scraping in PBS on ice. Then cells were washed once in PBS and resuspended in five cell volumes of buffer A (20 mM HEPES (pH 7.4), 40 mM KCl, 1.5 mM $MgCl_2$, 1 mM EDTA, 1 mM EGTA, 0.1 mM PMSF and 250 mM sucrose, 1 × protease inhibitors). Cells were then incubated for 30 min on ice in buffer A, and lysed by passage through a 22-gauge needle 30 times. Lysates were spun at 800*g* for 10 min to remove unbroken cells and nuclei. The post-nuclear supernatant was spun at 7,000*g* for 10 min, and the supernatant (S7) was re–spun at 20,000*g* for 10 min, whereas the pellet (P7) was resuspended in the same volume of buffer A. The resulting pellet (P20) was again resuspended in buffer A and the supernatant (S20) was re-spun at 100,000*g* for 1 h and the resulting supernatant (S100) was collected and the pellet (P100) was resuspended in the same volume of buffer A as before. All the pellets containing membrane proteins were washed with buffer A. To separate soluble and crude membrane fractions, cells were lysed in buffer A and intact cells, nuclei and cell debris were removed by centrifugation of the homogenate at 800*g* for 10 min at 4°C and then the supernatant was spun at 100,000*g* for 1 h at 4°C. The supernatant containing cytosolic proteins (soluble fraction) was collected. The pellets were washed with buffer A and were re-centrifuged at 100,000*g* for 1 h. The precipitate was the crude membrane fraction.

Immunostaining and confocal microscopy

Cells grown on coverslips were fixed for 15 min with 4% paraformaldehyde in PBS, permeabilized for 20 min in 0.1% Triton X-100 in PBS and blocked using 5% BSA for 1 h. Then, the cells were stained with the indicated primary antibodies, followed by incubation with fluorescent-conjugated goat anti-mouse IgG (Invitrogen). Nuclei were counterstained with DAPI (Cell Signaling). Slides were mounted using Fluorescence Mounting Medium (Dako). Images were captured at room temperature using a confocal microscope (Olympus Fluoview FV1000 Confocal System) with a 63 × water immersion objective and Olympus Fluoview software (Olympus). All confocal images are representative of three independent experiments.

Protein–lipid binding assay

Proteins were spotted on Membrane Lipid Strips (Echelon Biosciences) according to the manufacturer's instructions. To block non-specific binding, lipid strips were preincubated with binding assay buffer (3% fatty acid-free BSA (Sigma) in PBS) for 1 h at room temperature. Then the strips were incubated with protein (2 μg ml^{-1}) diluted in binding assay buffer for 1 h at room temperature and then washed three times (6 min each time) with wash buffer (0.1% Tween-20 in PBS). Membrane-bound proteins were detected by probing the lipid strips with corresponding primary antibodies diluted in binding assay buffer for 1 h at room temperature, followed by incubation for 1 h with horse- radish-peroxidase-conjugated secondary antibody diluted 1:2000 in binding assay buffer. After washing three times with wash buffer, proteins were visualized using a SuperSignal West Pico chemiluminescence ECL kit (Pierce).

Liposome binding assay

Liposomes were prepared by hydration of lipids (Avanti Polar Lipids) in buffer R (20 mM HEPES (pH 7.4), 150 mM NaCl) followed by extrusion through a 100-nm polycarbonate membrane (~24 passages). All liposomes were composed of a 4:1 molar ratio of distearoyl PC and PE, to which we added other phospholipids (PtdIns(4)P, PtdIns(4,5)P2, PS, PA) as indicated. For liposome binding assay, protein (0.1 μM) was incubated with liposomes in 100 μl of buffer R for 20 min at room temperature before sedimentation at 140,000*g* for 20 min at 4°C. Supernatants were removed immediately and the pellets were washed twice with buffer R and then resuspended in an equal volume of buffer. Proteins in both pellets and supernatant were then analysed by SDS–PAGE and immunoblot.

Liposome leakage assay

The leakage of liposomes encapsulating $TbCl_3$ was determined by an increase in fluorescence intensity when Tb^{3+} bound to DPA in the external buffer. Tb^{3+}-entrapped liposomes were prepared by hydration of the indicated lipids in buffer R containing 50 mM sodium citrate and 15 mM $TbCl_3$. Liposomes were washed twice to remove unincorporated $TbCl_3$. Then, Tb^{3+} entrapped liposomes were suspended in 100 μl buffer R supplemented with 50 μM of DPA and indicated GSDMD recombinant proteins were added. Fluorescence at 490 nm after excitation at 276 nm was continuously recorded for 9 min at 20 s intervals using a Biotek Synergy plate reader. At the end of the incubation, 0.1% Triton X-100 was

added to the medium to measure complete release of Tb^{3+}. The extent of liposome leakage was calculated by using the formula R: $t\,(\%) = 100 \times ((F_t - F_{t0})/(F_{t100} - F_{t0}))$, where F_{t0} is the initial fluorescence of the Tb^{3+} liposomes in the DPA-containing buffer at the time GSDMD recombinant proteins were added, F_t is the fluorescence signal recorded at individual time points, and F_t100 is the mean of the top-three fluorescence reads after adding 0.1% Triton X-100.

Preparation of unilamellar liposomes for reconstitution of GSDMD-NT pores

Synthetic 1,2-dioleoyl-*sn*-glycero-3-(phospho-L-serine) (DOPS), 1-palmitoyl-2-oleoyl-*sn*-glycero-3-phosphocholine (POPC) and 1,2-dioleoyl-*sn*-glycero-3-phosphoethanolamine (DOPE) (Avanti Polar Lipids) dissolved in chloroform were mixed in a glass tube at a mass ratio of 5:5:1, and the solvent was evaporated under a stream of N_2 gas. A buffer composed of 25 mM Tris-HCl (pH 8.0) and 150 mM NaCl was added to yield a final lipid concentration of 5 mM. The lipid suspension was then vortexed continuously for 5 min. To obtain unilamellar vesicles, liposomes were extruded with 21 passes through a mini-extruder device (Avanti) using membranes with 100 nm pores.

Reconstitution of GSDMD-NT pores on PS-containing liposomes

PS-containing liposomes (2 μmol) were incubated with 1 mg full length GSDMD and 0.3 mg caspase-11 for 4 h at 16°C. After incubation, the liposome–protein suspension was collected by ultracentrifugation at 60,000*g* for 30 min at 4°C. The pellets were washed twice with lysis buffer and then resuspended in 500 μl lysis buffer containing 0.5% C12E8 (Anatrace). After centrifugation for 30 min at 60,000*g*, the supernatant containing the solubilized GSDMD-NT pores was loaded in running buffer containing 0.5% C12E8 onto a Sepharose-6 gel filtration column. Fractions were analysed by SDS–PAGE and the fractions containing GSDMD-NT were pooled and imaged using negative staining electron microscopy.

Negative staining electron microscopy of GSDMD-NT pores

Copper grids (Electron Microscopy Sciences) coated with a layer of thin carbon were rendered hydrophilic immediately before use by glow-discharge in air with 25 mA current for 1 min. Liposome–protein suspensions (5 μl), or protein samples extracted from liposomes were loaded onto the grids, air dried for ~1 min and blotted, leaving a thin layer of sample on the grid surface. The grids were floated on a drop of staining solution containing 2% uranyl acetate for 60 s. After air drying, the grids were examined using a Tecnai G^2 Spirit BioTWIN electron microscope.

Bacterial growth assay

Colony-forming unit assays and turbidimetry were used to measure bacterial growth as previously described[11]. Briefly, for turbidimetry, bacteria were diluted (1:100) in bacterial culture medium following treatment and incubated with discontinuous shaking at 37°C in a 200 μl volume in flat-bottomed 96-well plates. Growth curves were monitored by reading absorbance at 600 nm over 16 h using a Spectra MAX 340 (Molecular Devices) or Synergy H4 Hybrid Multi-Mode Microplate Reader (BioTek). The time until the growth curves

reached a threshold OD_{600} of 0.05 above background was defined as the $T_{threshold}$. The ratio of $T_{threshold}$ (untreated): $T_{threshold}$ (treated) was used to quantify the change in bacterial growth.

LIVE/DEAD assay

Bacterial viability was assessed using the bacterial LIVE/DEAD assay (Invitrogen), following the manufacturer's recommendations. Briefly, bacteria were treated in the presence of 5 μM Syto-9 (Invitrogen) and 15 μM propidium iodide (Invitrogen). Treatment with 70% isopropanol served as a positive control. Fluorescence was visualized by confocal microscopy.

Fluorescent protein labelling and protein binding assay

Full-length and C-terminal GSDMD was labelled with AlexaFluor-488 using the Molecular Probes protein labelling kit. An aliquot of the labelled full-length protein was activated by incubating with active caspase-11 for 15 min at 37°C. *L. monocytogenes* expressing mCherry (a gift from J. Theriot, Stanford Medical School) were treated with PBS or with 500 nM AF488-labelled GSDMD that had been activated or not with caspase-11 or with GSDMD-CT for 30 min at 37°C. Bacteria were washed with 10 mM arginine in PBS for 10 min before fixation in 2% formalin in PBS. Slides were mounted with fluorescence mounting medium (Dako) and imaged using a fully motorized Axio Observer spinning disk microscope (Carl Zeiss Microimaging, Inc.) equipped with a cooled electron multiplication CCD camera with 512 × 512 resolution (Photometrics QuantEM, Tuscon, AZ) with excitation filters set at 405, 488, 561 and 640 nm and emission filter ranges of 430–475, 500–550, 589–625 and 680 nm long-pass, respectively. Images were analysed using SlideBook V5.0 (Intelligent Imaging Inc.) software. Third-dimensional image stacks were obtained along the *z* axis using the 63× oil immersion objective by acquiring sequential optical planes spaced 0.25 μm apart. Raw images were deconvolved using SlideBook.

Treatment of extracellular bacteria

HEK293T cells, cultured in antibiotic-free medium, were transfected with the indicated plasmids for 30 h before culture supernatants were collected and concentrated fivefold. iBMDMs, cultured in antibiotic-free medium, were transfected with LPS or Pam3CSK4 or incubated with LPS and nigericin for 3 h before culture supernatants were collected and used without concentration. Exponential phase bacteria were treated with the indicated antibiotic-free culture supernatants or recombinant proteins, which were cultured at 37°C for the indicated time. Treated bacteria were diluted in LB and plated on LB (*E. coli*, *S. aureus*) or brain–heart infusion agar (*L. monocytogenes*) agar plates to determine c.f.u., which were normalized to c.f.u. in control conditions.

Intracellular bacterial killing assay

HeLa cells or iBMDMs were transfected with indicated plasmids or siRNAs. Cells were infected with *L. monocytogenes* (multiplicity of infection, 10:1) 6 h after transfection of plasmids or 48 h after siRNA transfection. Cell plates were centrifuged at 1500 r.p.m. for 10 min, and placed at 37°C for 30 min before washing to remove extracellular bacteria. Cells

were lysed using 0.1% Triton-X100 at indicated time points after infection and supernatants were collected to determine bacterial titers by c.f.u. assay. For the nigericin experiment, iBMDMs were primed for 4 h with LPS (100 ng ml^{-1}) and then infected with *L. monocytogenes* as described above. After removing extracellular bacteria by washing, cells were treated or not with nigericin (20 μM) and 1 h later bacteria were collected as described above for c.f.u. assay.

Statistics

Student's *t*-test (two-tailed) was used for the statistical analysis of all experiments. *P* values <0.05 were considered significant.

Extended Data

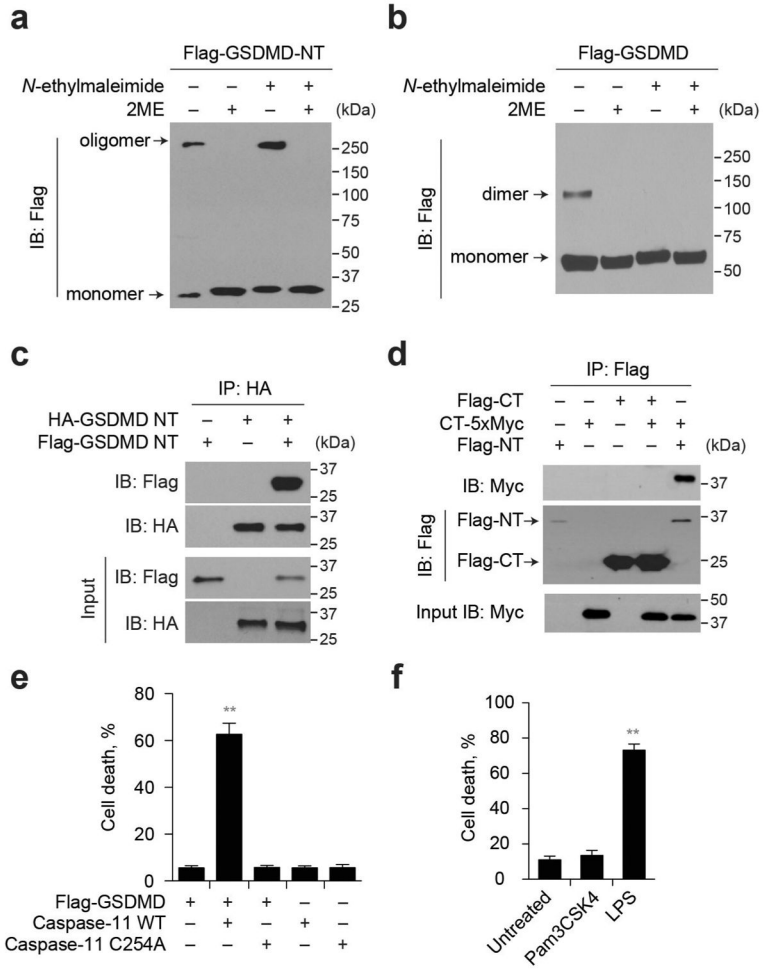

Extended Data Figure 1. GSDMD-NT oligomerizes and induces pyroptosis

a, b, HEK293T cells, transfected with Flag–GSDMD-NT (**a**) or Flag–GSDMD (**b**), were lysed with or without *N*-ethylmaleimide or 2ME, and analysed by SDS–PAGE and Flag immunoblot. **c**, Lysates of HEK293T cells, transfected with HA–GSDMD-NT and/or Flag–GSDMD-NT, were immunoprecipitated with anti-HA and analysed by immunoblot with the

indicated antibodies. **d**, HEK293T cells were transfected with the indicated plasmids. Cell lysates were immunoprecipitated with anti-Flag and analysed by immunoblot with the indicated antibodies. Flag–GSDMD-NT (Flag-NT) was expressed at considerably lower levels than GSDMD-CT-MYC (CT-MYC) or Flag–GSDMD-CT (Flag-CT), which accounts for the relative weak intensity of the corresponding bands on the middle blot. **e**, HEK293T cells, transiently transfected with the indicated plasmids, were assessed 16 h after transfection for cell death by CytoTox96 assay. **f**, Immortalized iBMDMs expressing Flag–GSDMD were electroporated with PBS, ultra LPS or Pam3CSK4, as a negative control for pyroptosis. 2 h later, cell death was determined by CytoTox96 assay. Graphs show the mean ± s.d. of triplicate wells and data shown are representative of three independent experiments. $^{**}P < 0.01$ (two-tailed *t*-test).

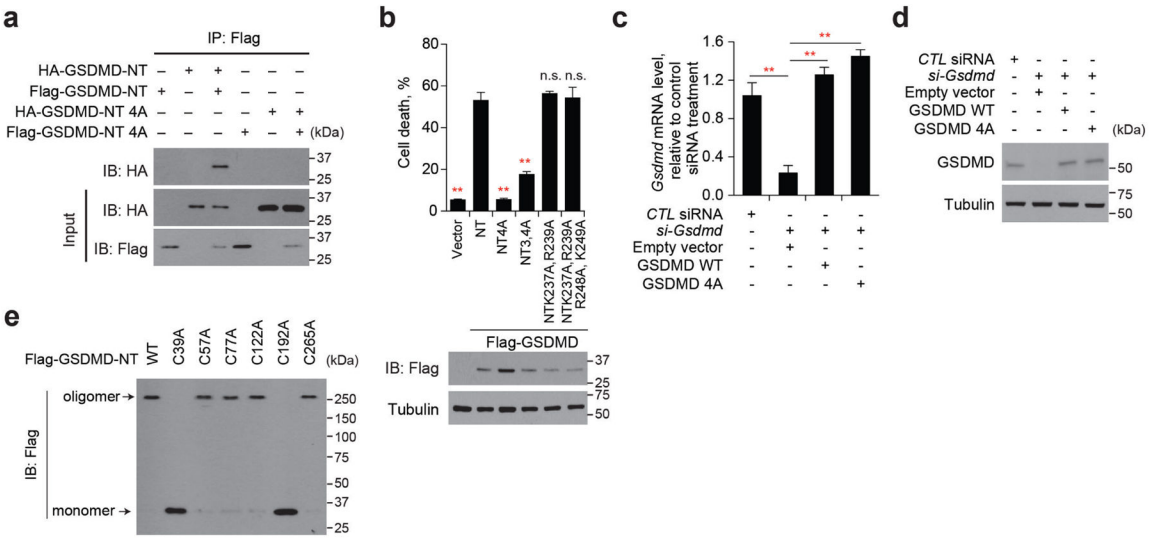

Extended Data Figure 2. Mutation of four positively charged residues in GSDMD-NT or of two cysteine residues disrupts pyroptosis

a, Lysates of HEK293T cells, transfected with the indicated plasmids, were immunoprecipitated with anti-Flag and analysed by immunoblot with the indicated antibodies. The 4A mutant of GSDMD-NT does not self-associate in multimers. **b**, Mutations in other basic residues do not affect pyroptosis. The indicated wild-type or mutated Flag–GSDMD-NT constructs were transiently expressed in HEK293T cells. Medium was collected 18 h after transfection and cell death was measured by CytoTox96 assay. **c, d**, Knockdown in immortalized iBMDMs of *Gsdmd* and ectopic expression of wild-type or 4A *Gsdmd* mRNA (**c**, assessed by qRT–PCR relative to *GAPDH*) and protein (**d**, relative to tubulin). These data for the cells used in the rescue experiment in Fig. 1h show that the ectopic proteins are expressed at similar levels as the endogenous protein. **e**, Replacement of Cys37 or Cys192 by Ala in GSDMD-NT disrupts oligomerization. Mean ± s. d. of three technical replicates and data shown are representative of three independent experiments (**b, c**). Statistical differences are calculated by two-tailed *t*-test (in **b**, compared to samples transfected to express wild-type GSDMD-NT); $^{**}P < 0.01$ (two-tailed *t*-test).

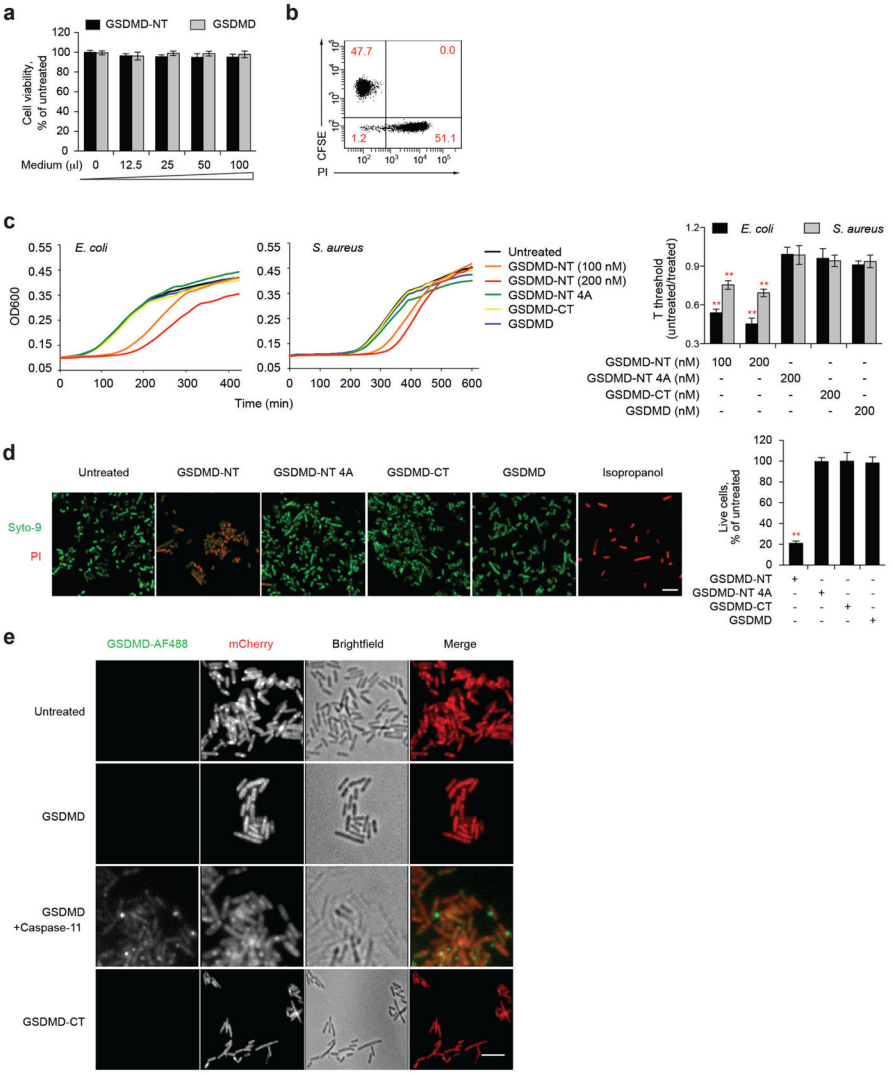

Extended Data Figure 3. Treatment with GSDMD-NT reduces bacterial viability, but does not affect the viability of mammalian cells

a, Antibiotic-free culture supernatants (concentrated fivefold) from transfected HEK293T cells, collected 30 h after transfection, were added to iBMDMs, which were cultured at 37 °C in 200 µl final volume for 6 h before measuring viability by CellTiter-Glo. **b**, HEK293T cells, transfected with Flag–GSDMD-NT 6 h earlier, were mixed with an equal number of CFSE-labelled untransfected HEK293T cells and incubated for 18 h before assessing cell death by propidium iodide staining and flow cytometry. **c**, *E. coli* and *S. aureus* were untreated or treated with recombinant GSDMD, wild-type or 4A-mutant GSDMD-NT, or GSDMD-CT (200 nM or indicated concentrations) for 20 min before samples were collected and bacterial growth was assessed by monitoring turbidity by optical density (representative experiments, left). The time to reach OD_{600} of 0.05 above background, which is a quantitative measure of the lag in detectable growth because of fewer viable bacteria, was defined as $T_{threshold}$ (right). The right graph shows the mean ± s.d. of three technical replicates. **d**, Bacterial viability after 20 min incubation with indicated

proteins (200 nM) or isopropanol. Syto-9 enters live and dead bacteria, PI only enters dead bacteria (representative images, left; percent live cells, right). **e**, Fluorescence microscopy of mCherry-expressing *L. monocytogenes* incubated with AlexaFluor 488-GSDMD (activated or not with caspase-11) or AlexaFluor488-GSDMD-CT for 30 min at 37 °C. Data shown are representative of results of three independent experiments. Statistical differences are relative to untreated samples; $^{**}P < 0.01$ (two-tailed *t*-test). Scale bars, 5 μm.

Supplementary Material

Refer to Web version on PubMed Central for supplementary material.

Acknowledgments

This work was supported by US NIH grant R01AI123265 (J.L.).

References

1. Shi J, et al. Cleavage of GSDMD by inflammatory caspases determines pyroptotic cell death. Nature. 2015; 526:660–665. [PubMed: 26375003]
2. Kayagaki N, et al. Caspase-11 cleaves gasdermin D for non-canonical inflammasome signalling. Nature. 2015; 526:666–671. [PubMed: 26375259]
3. Rathinam VA, et al. TRIF licenses caspase-11-dependent NLRP3 inflammasome activation by gram-negative bacteria. Cell. 2012; 150:606–619. [PubMed: 22819539]
4. Hagar JA, Powell DA, Aachoui Y, Ernst RK, Miao EA. Cytoplasmic LPS activates caspase-11: implications in TLR4-independent endotoxic shock. Science. 2013; 341:1250–1253. [PubMed: 24031018]
5. Law RH, et al. The structural basis for membrane binding and pore formation by lymphocyte perforin. Nature. 2010; 468:447–451. [PubMed: 21037563]
6. Montal M. Design of molecular function: channels of communication. Annu Rev Biophys Biomol Struct. 1995; 24:31–57. [PubMed: 7663119]
7. Rosado CJ, et al. The MACPF/CDC family of pore-forming toxins. Cell Microbiol. 2008; 10:1765–1774. [PubMed: 18564372]
8. Geourjon C, Deléage G. SOPMA: significant improvements in protein secondary structure prediction by consensus prediction from multiple alignments. Comput Appl Biosci. 1995; 11:681–684. [PubMed: 8808585]
9. Bordier C. Phase separation of integral membrane proteins in Triton X-114 solution. J Biol Chem. 1981; 256:1604–1607. [PubMed: 6257680]
10. Dotiwala F, et al. Killer lymphocytes use granulysin, perforin and granzymes to kill intracellular parasites. Nat Med. 2016; 22:210–216. [PubMed: 26752517]
11. Walch M, et al. Cytotoxic cells kill intracellular bacteria through granulysin-mediated delivery of granzymes. Cell. 2014; 157:1309–1323. [PubMed: 24906149]
12. van Meer G, Voelker DR, Feigenson GW. Membrane lipids: where they are and how they behave. Nat Rev Mol Cell Biol. 2008; 9:112–124. [PubMed: 18216768]
13. Leventis PA, Grinstein S. The distribution and function of phosphatidylserine in cellular membranes. Annu Rev Biophys. 2010; 39:407–427. [PubMed: 20192774]
14. Schlame M. Cardiolipin synthesis for the assembly of bacterial and mitochondrial membranes. J Lipid Res. 2008; 49:1607–1620. [PubMed: 18077827]
15. Pasparakis M, Vandenabeele P. Necroptosis and its role in inflammation. Nature. 2015; 517:311–320. [PubMed: 25592536]
16. Dondelinger Y, et al. MLKL compromises plasma membrane integrity by binding to phosphatidylinositol phosphates. Cell Reports. 2014; 7:971–981. [PubMed: 24813885]

17. Wang H, et al. Mixed lineage kinase domain-like protein MLKL causes necrotic membrane disruption upon phosphorylation by RIP3. Mol Cell. 2014; 54:133–146. [PubMed: 24703947]
18. Sun L, et al. Mixed lineage kinase domain-like protein mediates necrosis signaling downstream of RIP3 kinase. Cell. 2012; 148:213–227. [PubMed: 22265413]
19. Wilschut J, Papahadjopoulos D. Ca^{2+}-induced fusion of phospholipid vesicles monitored by mixing of aqueous contents. Nature. 1979; 281:690–692. [PubMed: 551288]
20. He WT, et al. Gasdermin D is an executor of pyroptosis and required for interleukin-1β secretion. Cell Res. 2015; 25:1285–1298. [PubMed: 26611636]
21. Finzel BC, et al. Crystal structure of recombinant human interleukin-1β at 2.0 Å resolution. J Mol Biol. 1989; 209:779–791. [PubMed: 2585509]
22. Lamkanfi M, Dixit VM. Mechanisms and functions of inflammasomes. Cell. 2014; 157:1013–1022. [PubMed: 24855941]
23. Rühl S, Broz P. Caspase-11 activates a canonical NLRP3 inflammasome by promoting K^+ efflux. Eur J Immunol. 2015; 45:2927–2936. [PubMed: 26173909]
24. Warren SE, Mao DP, Rodriguez AE, Miao EA, Aderem A. Multiple Nod-like receptors activate caspase 1 during *Listeria monocytogenes* infection. J Immunol. 2008; 180:7558–7564. [PubMed: 18490757]
25. Cervantes J, Nagata T, Uchijima M, Shibata K, Koide Y. Intracytosolic *Listeria monocytogenes* induces cell death through caspase-1 activation in murine macrophages. Cell Microbiol. 2008; 10:41–52. [PubMed: 17662073]
26. Aachoui Y, et al. Caspase-11 protects against bacteria that escape the vacuole. Science. 2013; 339:975–978. [PubMed: 23348507]
27. Wu J, Fernandes-Alnemri T, Alnemri ES. Involvement of the AIM2, NLRC4, and NLRP3 inflammasomes in caspase-1 activation by Listeria monocytogenes. J Clin Immunol. 2010; 30:693–702. [PubMed: 20490635]
28. Sauer JD, et al. Listeria monocytogenes triggers AIM2-mediated pyroptosis upon infrequent bacteriolysis in the macrophage cytosol. Cell Host Microbe. 2010; 7:412–419. [PubMed: 20417169]
29. Miao EA, et al. Caspase-1-induced pyroptosis is an innate immune effector mechanism against intracellular bacteria. Nat Immunol. 2010; 11:1136–1142. [PubMed: 21057511]
30. Thiery J, Walch M, Jensen DK, Martinvalet D, Lieberman J. Isolation of cytotoxic T cell and NK granules and purification of their effector proteins. Curr Protoc Cell Biol. 2010; 47:3.37:3.37.1–3.37.29.

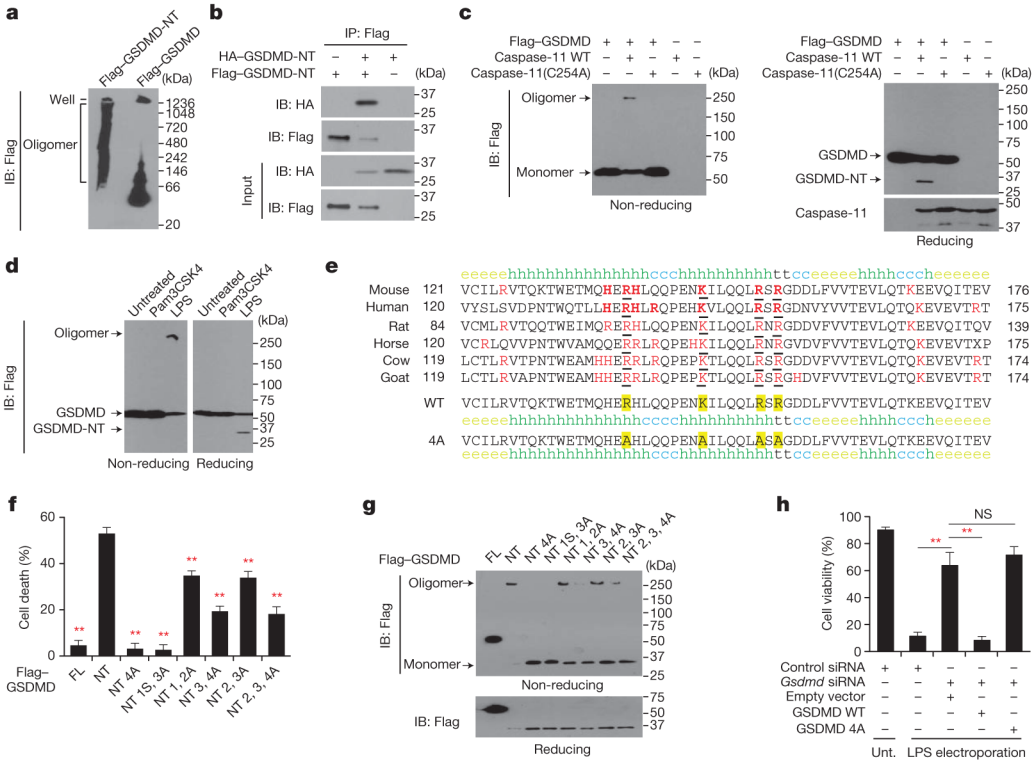

Figure 1. GSDMD-NT forms oligomers, disrupted by mutation of four positively charged residues

a, HEK293T cells, transfected with indicated plasmids, lysed under non-reducing conditions, were resolved on a native gel, immunoblotted for Flag. **b**, Flag immunoprecipitation of lysates of HEK293T cells, transfected with HA–GSDMD-NT and/or Flag–GSDMD-NT, were analysed by immunoblot. **c**, HEK293T cells, transiently transfected with indicated plasmids, were assessed 16 h after transfection for oligomer formation by Flag immunoblot of non-reducing (left) or reducing (right) gels. The reducing gel was also blotted for caspase-11. **d**, iBMDMs expressing Flag–GSDMD were electroporated with phosphate-buffered solution (PBS), LPS or Pam3CSK4 and analysed 2 h later by Flag immunoblot. **e**, The cluster of four evolutionarily conserved, positively charged amino acids (red and underlined) in GSDMD-NT were mutated to Ala. Secondary structures of the wild-type and 4A-mutated mouse GSDMD fragment were predicted using the SOPMA algorithm. h, helix; e, sheet; t, turn; c, coil. **f, g**, Mutations of mouse GSDMD-NT block GSDMD-NT-mediated pyroptosis (**f**) and oligomerization (**g**). The first to fourth amino acids (R138/K146/R152/R154) were mutated to Ala. The mutated residues are indicated, i.e. in NT4A, all 4 residues are mutated; in NT 3, 4A, the 3rd and 4th residues are mutated. In NT1S3A, R138 was mutated to Ser, the other three residues were mutated to Ala. FL, full-length GSDMD; NT, GSDMD-NT. HEK293T cells, transfected with wild-type (WT) or mutated GSDMD-NT, were analysed 18 h later for cell death (CytoTox96 assay) and GSDMD oligomerization (Flag immunoblot). GSDMD-NT monomer and oligomer are indicated. **h**, iBMDMs, co-transfected with control or *Gsdmd* siRNA and the indicated siRNA-resistant *Gsdmd* expression plasmids, were electroporated with LPS. The number of surviving cells was determined by CellTiter-Glo assay 2.5 h later. Mean ±s.d. of three

technical replicates from one of three independent experiments are shown (**f, h**). Statistical differences are relative to Flag–GSDMD-NT-expressing samples (**f**). $^{**}P<0.01$ (two-tailed *t*-test). NS, not significant; unt., not transfected with LPS.

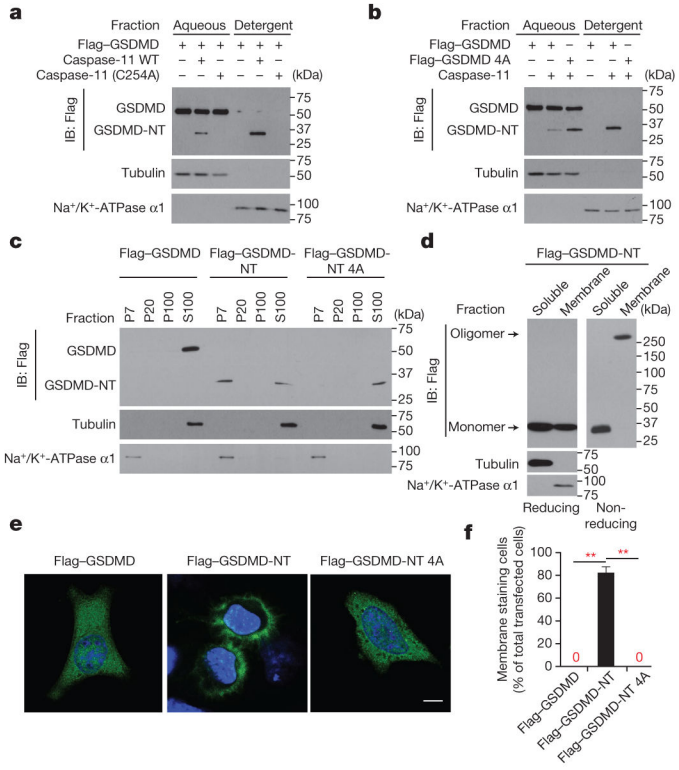

Figure 2. GSDMD-NT localizes to the plasma membrane

a, b, Lysates of HEK293T cells, transfected with indicated plasmids for 16 h, were separated into aqueous and detergent phases using Triton X-114, and analysed by immunoblot probed for Flag, tubulin, or Na^+/K^+-ATPase α1. **c**, HEK293T cells, transfected with indicated plasmids for 16 h, were separated into P7 (heavy membrane), P20 (light membrane), P100 (insoluble cytosol) and S100 (soluble cytosol) fractions and analysed by immunoblot with indicated antibodies. **d**, Soluble and crude membrane fractions of HEK293T cells, transfected to express Flag–GSDMD-NT, were analysed by immunoblot as indicated. **e, f**, Representative confocal microscopy images (**e**) and quantification (**f**) of distribution of ectopic Flag–GSDMD, Flag–GSDMD-NT and Flag–GSDMD-NT 4A (green) in HeLa cells co-stained with DAPI (blue). The ratio of cells with membrane versus cytosolic Flag staining was calculated by counting 10 high-power fields for each sample in 5 independent experiments (**f**). $^{**}P < 0.0001$ (paired *t*-test). Scale bar, 20 μm. Data are representative of three independent experiments (**a–d**).

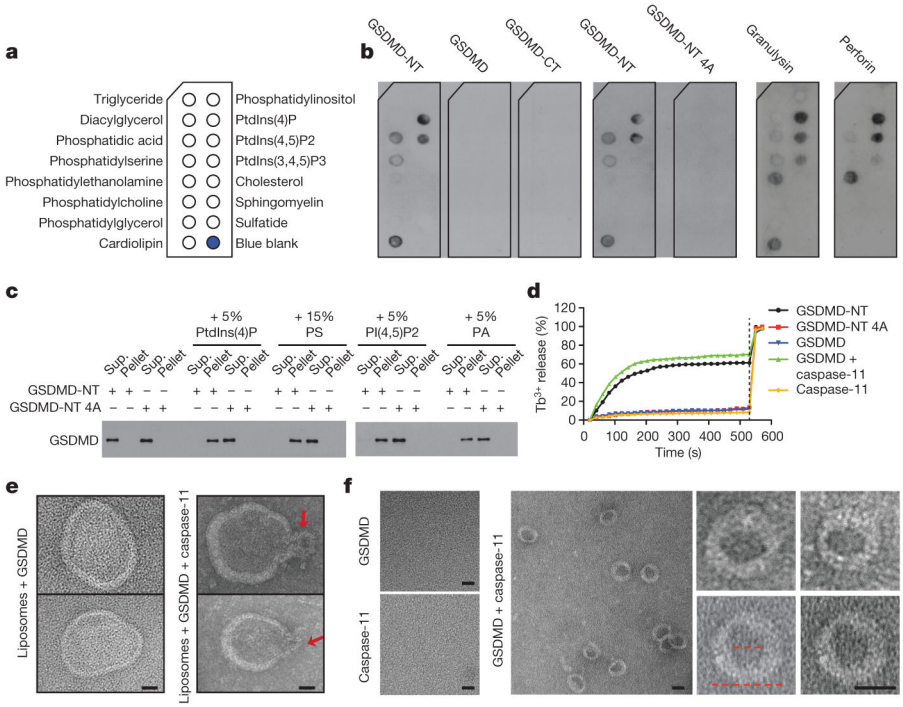

Figure 3. N-terminal gasdermin D binds to phosphatidyl serine and cardiolipin and forms pores on liposomes

a, b, Membranes displaying lipids (**a**) were incubated with indicated proteins and binding was assessed by blotting for GSDMD, perforin or granulysin (**b**). **c**, Wild-type or 4A-mutant GSDMD-NT binding to PC–PE liposomes containing additional indicated phospholipids (molar proportion of added lipid indicated) was analysed by SDS–PAGE and GSDMD immunoblot. **d**, Liposome leakage was monitored by terbium (Tb^{3+}) fluorescence after incubation with the indicated GSDMD protein ±caspase-11. Detergent was added after 9 min (dotted line). **e**, Negative staining electron microscopy images of PE–PC–PS liposomes treated with GSDMD (left) or caspase-11-activated GSDMD (right). Arrows indicate potential side views of GSDMD-NT pores. **f**, Negative staining electron microscopy images of GSDMD-NT pores formed in PS-containing liposomes and extracted by detergent. The left image of pores formed by GSDMD and caspase-11 shows a field with multiple rings, whereas the right images show enlarged single rings. The inner and outer diameters (red dotted lines) are approximately 15 nm and 32 nm, respectively. Data are representative of three independent experiments. Scale bars, 20 nm

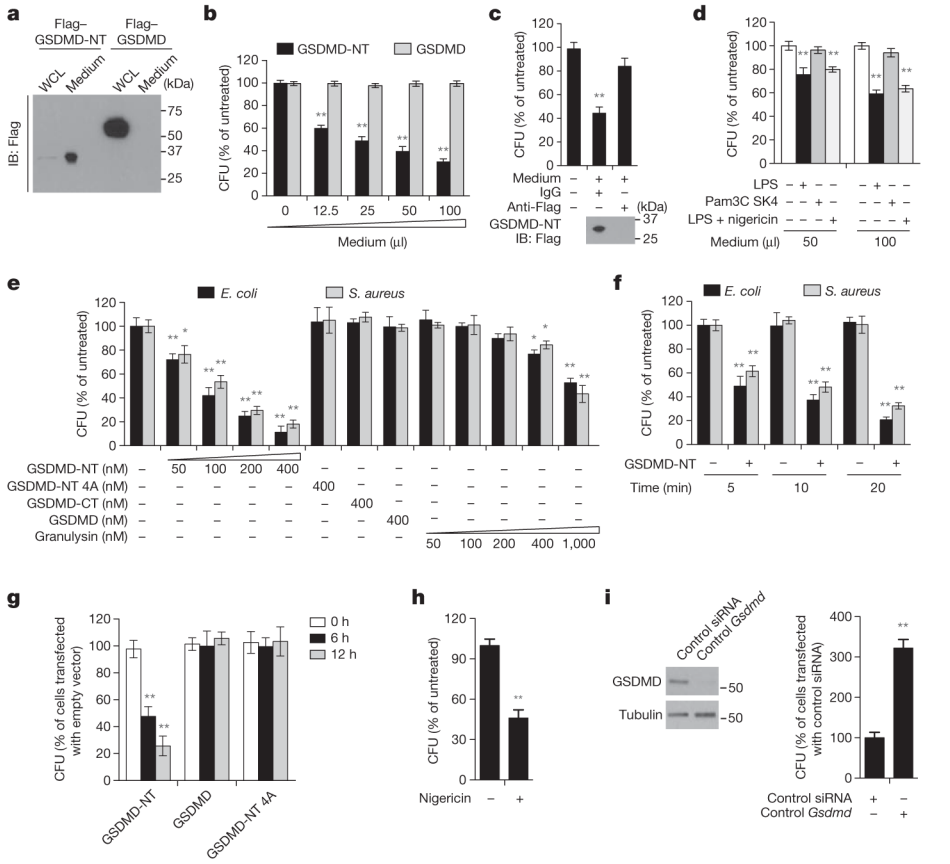

Figure 4. GSDMD-NT kills bacteria

a, Culture supernatants and whole-cell lysates (WCL) of HEK293T cells, transiently expressing Flag–GSDMD-NT or Flag–GSDMD for 20 h, were analysed by Flag immunoblot of reducing gel. **b**, Antibiotic-free culture supernatants (concentrated fivefold) from transfected HEK293T cells, collected 30 h after transfection, were added to *E. coli*, which were cultured at 37 °C in 200 μl final volume for 30 min before measuring c.f.u. **c**, The concentrated culture medium from Flag–GSDMD-NT-expressing HEK293T cells was immunodepleted with anti-Flag or control IgG, before adding to *E. coli*, as in **b**. Lower panel, Flag immunoblot. **d**, *L. monocytogenes* were incubated at 37 °C for 30 min with antibiotic-free culture supernatants from iBMDMs, transfected with LPS or Pam3CSK4 or incubated with LPS and nigericin for 3 h, before assessing c.f.u. **e, f**, *E. coli* and *S. aureus* were treated with the indicated proteins for 20 min (**e**) or with 200 nM wild-type GSDMD-NT for the indicated times (**f**) before measuring c.f.u. **g**, HeLa cells, transfected for 6 h to express the indicated proteins, were infected with *L. monocytogenes* for the indicated times before cells were lysed to analyse intracellular c.f.u. **h**, LPS-primed-iBMDMs infected with *L. monocytogenes*, were treated or not with nigericin for 1 h before bacteria were collected and c.f.u. was analysed. Nigericin had no effect on cell-free bacteria (not shown). **i**, iBMDMs, transfected with control or *Gsdmd* siRNA, were infected with *L. monocytogenes* and assessed for intracellular c.f.u. 12 h later. GSDMD immunoblot, left. Shown are mean ± s.d. of triplicates of one experiment of three (**b, d–f, h**) or two (**c, g, i**) independent

experiments. Statistical differences compared to untreated control samples (two-tailed *t*-test); $*P<0.05$, $**P<0.01$.